# Biochemical Basis of Polyvalency as a Strategy for Enhancing the Efficacy of P-Glycoprotein (ABCB1) Modulators: Stipiamide Homodimers Separated with Defined-Length Spacers Reverse Drug Efflux with Greater Efficacy

Zuben E. Sauna,[‡] Merritt B. Andrus,[§] Timothy M. Turner,[§] and Suresh V. Ambudkar*[,‡]

*Laboratory of Cell Biology, Center for Cancer Research, National Cancer Institute, National Institutes of Health, Bethesda, Maryland 20892-4254, and Department of Chemistry and Biochemistry, Brigham Young University, Provo, Utah 84602-5700*

*Received November 4, 2003; Revised Manuscript Received December 24, 2003*

ABSTRACT: Human P-glycoprotein (Pgp) is as an ATP-dependent efflux pump for a variety of chemotherapeutic drugs. The aim of this study is to evaluate whether Pgp modulators can be engineered to exhibit high-affinity binding using polyvalency. Five bivalent homodimeric polyenes based on stipiamide linked with polyethylene glycol ethers in the range of 3−50 Å were synthesized and quantitatively characterized for their effect on Pgp function. The stipiamide homodimers displaced [$^{125}$I]iodoarylazidoprazoin (IAAP), an analogue of the Pgp substrate prazosin. A minimal spacer of 11 Å is necessary for inhibition of IAAP labeling, beyond which there is an inverse correlation between the length of the spacer and the $IC_{50}$ for the displacement of IAAP. ATP hydrolysis by Pgp on the other hand is stimulated by the dimers with spacers of up to 22 Å, whereas dimers with longer spacers inhibit ATP hydrolysis. Finally, the homodimers reverse Pgp-mediated drug efflux in intact cells overexpressing Pgp, and 11 Å is a threshold beyond which the effectiveness of the homodimers increases exponentially and levels off at 33 Å. We demonstrate that dimerization and identification of an optimal spacer length increase by 11-fold the affinity of stipiamide, and this is reflected in the efficacy with which Pgp-mediated drug efflux is reversed. These results suggest that polyvalency could be a useful strategy for the development of more potent Pgp modulators.

P-Glycoprotein (Pgp)[1] belongs to the ATP binding cassette (ABC) superfamily of transport proteins, characterized by two homologous halves containing six transmembrane helices and one nucleotide binding site in each half (*1*, *2*). Pgp confers drug resistance to tumor cells by extruding cytotoxic natural product hydrophobic drugs using the energy of ATP hydrolysis (*3*, *4*). Pgp interacts with a diverse set of other lipophilic compounds, and the only feature common to Pgp−drug substrates appeared to be that they are all hydrophobic with a molecular mass of 300−2000 kDa (*5*). A more detailed study by Seelig and co-workers of the biophysical characteristics of Pgp substrates suggested that Pgp−drug interactions may be a function of the spatial separation of electron donor groups (*6*, *7*). In addition, other studies have demonstrated that the number and strength of hydrogen bonds also contribute to the interaction of Pgp and drug substrates (*8*). Although there have been several generations of Pgp modulators in development, reversing Pgp-mediated MDR in the clinic has met with very limited success (*9*, *10*). This is a significant issue in drug development, considering the importance of Pgp in cancer chemotherapy (*11*).

A unique approach to developing Pgp modulators involves exploiting a known MDR modulator as a molecular scaffold and generating a large pool of potential modulators using solid-phase combinatorial chemistry (*12*−*14*). The fungal antibiotic stipiamide was first described as a natural product modulator of Pgp (*15*). Subsequently, stipiamide was chemically synthesized as was a more potent and less toxic compound 6,7-dehydrostipiamide (*16*). A solution-phase combinatorial library of dehydrostipiamide compounds was generated and was screened to identify several potent compounds (*12*−*14*). Finally, a series of five bivalent homodimeric polyenes based on stipiamide were generated using polyethylene glycol ethers (PEG ethers) as spacers (*17*) as a means of evaluating polyvalency as a strategy for enhancing the efficacy of Pgp modulators.

Work from several laboratories has indicated that there are at least two, and plausibly several, drug binding sites associated with Pgp (*18*−*21*). Furthermore, detailed kinetic analyses of of Pgp−drug interactions by Stein and co-workers suggest that the behavior of some Pgp modulators (e.g., vinblastine) is best described by a Hill number of 2. This observation led them to postulate that pairs of vinblastine molecules cooperate at the active site of Pgp (*22*, *23*). There is considerable potential in augmenting the interactions of such a molecule with its ligand by introducing polyvalency

* To whom correspondence should be addressed: Laboratory of Cell Biology, Center for Cancer Research, NCI, NIH, Building 37, Room 1B-22, 37 Convent Dr., Bethesda, MD 20892-4254. E-mail: ambudkar@helix.nih.gov.

‡ National Institutes of Health.

§ Brigham Young University.

[1] Abbreviations: ABC, ATP-binding cassette; IAAP, [$^{125}$I]iodoarylazidoprazosin; NBD, nucleotide-binding domain; PAGE, polyacrylamide gel electrophoresis; PEG, polyethylene glycol; Pgp, P-glycoprotein; Vi, orthovanadate.

10.1021/bi035965k CCC: $27.50 
Published on Web 02/06/2004

in the ligand (*24*, *25*). Both the theoretical basis (*26*, *27*) and application of the polyvalency in drug design (*28*) have been studied. Essentially, polyvalency exploits cooperativity effects during molecular recognition and binding, wherein numerous weak interactions operate simultaneously. This results in a polyvalent ligand binding more tightly than the equivalent monovalent system. The most spectacular practical applications of polyvalency have been the polyvalent derivatives of vancomycin (*26*, *27*). Using an artificial vancomycin·D-Ala-D-Ala system, the binding was not only significantly tighter than that of the monovalent equivalent but also 25 times tighter than the biotin−avidin affinity, the gold standard for small molecule tight binding (*26*). Though several groups have attempted to elucidate the thermodynamic, kinetic, and structural basis of these high-affinity systems (*29*, *30*), they are not completely understood. Empirical evidence moreover suggests that in addition to multivalency *per se* other factors such as the length of the spacer between the monomers and the rigidity of the ligand play a significant role in the development of high-affinity polyvalent ligands.

In this study, we have evaluated the five bivalent homodimers of stipiamide vis-à-vis their affinity for Pgp, their ability to stimulate Pgp-mediated ATP hydrolysis, and their capacity to reverse drug efflux by Pgp. We show that dimerization coupled with the insertion of a spacer of the appropriate length can enhance the affinity of stipiamide almost 70-fold. The effects on the other functional characteristics of Pgp are consistent with the change in affinity. Finally, our results indicate that the series of stipiamide dimers can be used to understand the molecular dimensions and nature of the human Pgp drug binding site.

## EXPERIMENTAL PROCEDURES

*Chemicals.* Bodipy-FL-prazosin was purchased from Molecular Probes, Inc. (Eugene, OR). Cyclosporin A was purchased from Calbiochem (San Diego, CA). [$^{125}$I]Iodoarylazidoprazosin (IAAP, 2200 Ci/mmol) was obtained from Perkin-Elmer Life Sciences (Boston, MA). [α-$^{32}$P]-8-AzidoATP (15−20 Ci/mmol) and 8-azidoATP were purchased from Affinity Labeling Technologies, Inc. (Lexington, KY). All other chemicals were obtained from Sigma Chemical Co. (St. Louis, MO).

*Synthesis of the Stipiamide Monomer and Homodimers.* We generated bivalent homodimers of stipiamide linked with PEG ethers as described previously (*17*). PEG ethers were used to generate five different dimers. As the monomer control, we used the stipiamide monomer with a polyethylene tail, and the homodimers had spacers of 0, 2, 5, 8, and 12 ethyl ethers which correspond to 3, 11, 22, 35, and 50 Å, respectively. The chemical linkage for the homodimer with no spacer was a simple ethyl group.

*Drug Accumulation Assays by Flow Cytometry.* The fluorescent drug accumulation assay was performed in intact NIH-3T3 cells or in NIH-3T3 cells transfected with the human *MDR*1 gene (*31*). The human Pgp-expressing cells do not overexpress mouse Pgp. Control or Pgp-expressing cells (250 000 per assay) were suspended in IMDM containing 5% FBS. Cells were untreated or exposed to the modulators at the concentrations indicated in the figure legends for 5 min at 37 °C. Bodipy-Prazosin was then added to the samples at a final concentration of 0.5 μM, and the mixtures were incubated at 37 °C for an additional 40 min in the dark. All assays were carried out in a reaction mixture of 4.5 mL. At the end of the 40 min incubation, the cells were centrifuged for 10 min at 500*g* and transferred to ice. The cells were resuspended in PBS containing 0.1% BSA and analyzed on a FACSort flow cytometer using CellQuest software (FACS system from Becton Dickinson, San Jose, CA) as described previously (*32*−*34*).

*Preparation of Crude Membranes from High Five Insect Cells Infected with Recombinant Baculovirus Carrying the Human MDR1 Gene.* High Five insect cells (Invitrogen, Carlsbad, CA) were infected with the recombinant baculovirus carrying the human *MDR*1 cDNA with a six-histidine tag at the C-terminal end [BV-*MDR*1 (H6)] as described previously (*35*). Crude membranes were prepared as described previously (*35*) and stored at −70 °C.

*Photoaffinity Labeling with IAAP.* The crude membranes (50 μg of protein) were incubated with increasing concentrations of the stipiamide monomer, and each of the dimers was incubated for 3 min at room temperature in 50 mM Tris-HCl (pH 7.5). IAAP (8−10 nM) was then added followed by incubation for an additional 5 min under subdued light. The samples were then illuminated with a UV lamp assembly (PGC Scientifics, Gaithersburg, MD) fitted with two black light (self-filtering) UV-A long wave-F15T8BLB tubes (365 nm) for 10 min at room temperature (21−23 °C). SDS−PAGE sample buffer was added to each sample, and the samples were incubated at room temperature for 30 min and electrophoresed on an 8% Tris-glycine gel at a constant voltage. In some experiments (as indicated in the figure legend), intact NIH-3T3 cells expressing Pgp were also labeled with IAAP; 200 000 cells in IMDM containing 5% FBS were incubated with IAAP (10 nM) for 5 min under subdued light, and exposed to UV light (365 nm) for 10 min at 21−23 °C. The cells were centrifuged at 500*g* for 5 min, and the supernatant was discarded. Cells were then resuspended in 100 μL of TD buffer [10 mM Tris-HCl (pH 8.0), 0.1% Triton X-100 (v/v), 10 mM $MgSO_4$, 2 mM $CaCl_2$, 1% (v/v) aprotinin, 2 mM AEBSF, 1 mM DTT, and 20 μg/mL micrococcal nuclease], incubated at 37 °C for 5 min, and quick-frozen in dry ice. The samples were then thawed and sonicated thrice in a bath sonicator (1 min per sonication); gel loading buffer was added to the cells, and the cells were electrophoresed. Gels were dried and exposed to Bio-Max MR film (Eastman Kodak, Rochester, NY) at −70 °C for 12−24 h. The radioactivity incorporated into the Pgp band was estimated using the STORM 860 phosphorimager system (Molecular Dynamics, Sunnyvale, CA) using ImageQuaNT. In phosphorimage analyses, radioactivity was obtained as arbitrary units.

*ATPase Assay.* The Vi-sensitive ATPase activity of wild-type and mutant Pgps was determined by using the $P_i$ release assay as described previously (*35*−*37*).

*Binding of [α−$^{32}$P]-8-AzidoATP to Pgp.* Crude membranes (1 mg/mL) were incubated in the ATPase assay buffer containing 10 μM [α-$^{32}$P]-8-azidoATP (containing 10 μCi/nmol) in the dark at 4 °C for 5 min in the presence or absence of 25 μM stipiamide monomer and each of the stipiamide dimers. The samples were then illuminated with a UV lamp assembly (365 nm) as described above for 10 min on ice (4 °C). Ice-cold ATP (12.5 mM) was added to displace excess noncovalently bound [α-$^{32}$P]-8-azidoATP. Following SDS−

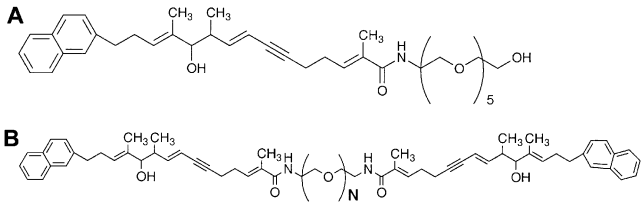

FIGURE 1: Structures of the stipiamide monomer and the dimers. (A) Structure of the stipiamide monomer with a PEG ether tail used as a control in all the experiments. (B) Structure of the stipiamide homodimeric dimers, where *N* refers to the number of PEG ether groups used as spacers between the two monomers. For these studies, five homodimers were synthesized with linkers of 3, 11, 22, 35, and 50 Å.

PAGE on an 8% Tris-glycine gel at a constant voltage, gels were dried and exposed to Bio-Max MR film at −70 °C for 12−24 h.

## RESULTS

*Synthesis of Stipiamide Dimers.* Though the precise number and organization of the drug−substrate binding sites of Pgp are unclear, there is a general consensus that Pgp has multiple binding sites (*18*−*21*, *38*, *39*) and that two molecules of some modulators may exhibit cooperativity (*22*). Several groups have successfully used polyvalency to increase the binding and efficiency of drugs when the target protein has multiple binding sites (*25*, *28*, *40*, *41*). Loose interactions occur because the enthalpy of the protein−ligand interaction (the sum of the favorable bond interactions) can be countered by the entropy arising out of the residual motion in the molecule (*26*). By generating a polyvalent ligand for a protein with multiple binding sites, we aimed to overcome this entropy by allowing numerous weak interactions to occur simultaneously. The low affinity of Pgp for modulators has been an impediment to the development of clinical interventions (*9*). In recent years, several modulators of Pgp that have high potency and specificity such as XR 9576 (*42*), LY 335979 (*43*), and GF 120918 (*44*) are in clinical trials. The evidence of the existence of several drug binding sites associated with Pgp suggests that polyvalency may be an valuable approach to enhancing the efficacy of Pgp modulators. In this study, we have used bivalent homodimers of stipiamide as a strategy for increasing the affinity of Pgp modulators. Besides polyvalency *per se*, the length and nature of the linker between the monomers are critical for the success of this approach. Thus, we used a set of six molecules in this study which were synthesized as described previously (*17*). As a control, we used a stipiamide monomer with a polyethylene tail (Figure 1A) and five dimers which differ only in the length of an ethylene glycol ether (Figure 1B).

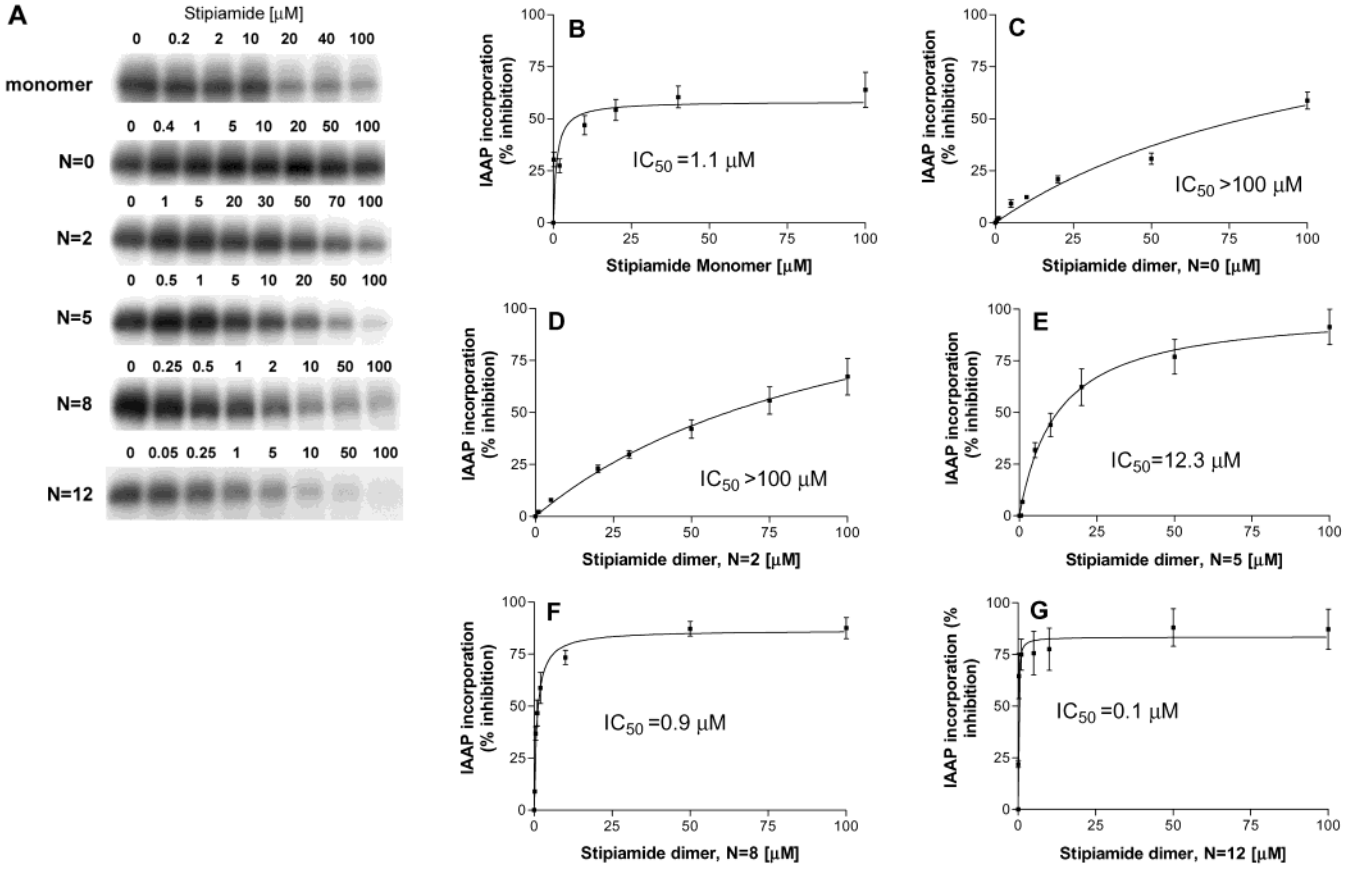


FIGURE 2: Effect of the stipiamide monomer and dimers on the binding of IAAP to Pgp. The binding of IAAP (5−10 nM) to Pgp was monitored as described in Experimental Procedures to determine the effect of increasing concentrations (ranging from 0 to 100 $\mu$M) of the stipiamide monomer and the homodimers separated with 3, 11, 22, 35, and 50 Å linkers. (A) The autoradiogram depicts the Pgp band in the presence of the increasing concentrations of the stipiamides. As the stipiamides displaced IAAP with different affinities, different concentrations were used, and these are depicted in the graphs (B−G). (B−G) Following SDS−PAGE, the gels were dried and the radioactivity incorporated into the Pgp band was quantified using the STORM 860 phosphorimager system and ImageQuaNT. The graphs depict the percent inhibition of [$^{125}$ I]IAAP incorporation in the Pgp band as a function of increasing concentrations of the stipiamide monomer and dimers (the individual dimers are identified on the plot). The data represent the means ± the standard deviation ($N = 3$). The $IC_{50}$ values were obtained by fitting the data to the Henri−Michaelis−Menten equation using the curve fitting software GraphPad Prism (version 2.0).

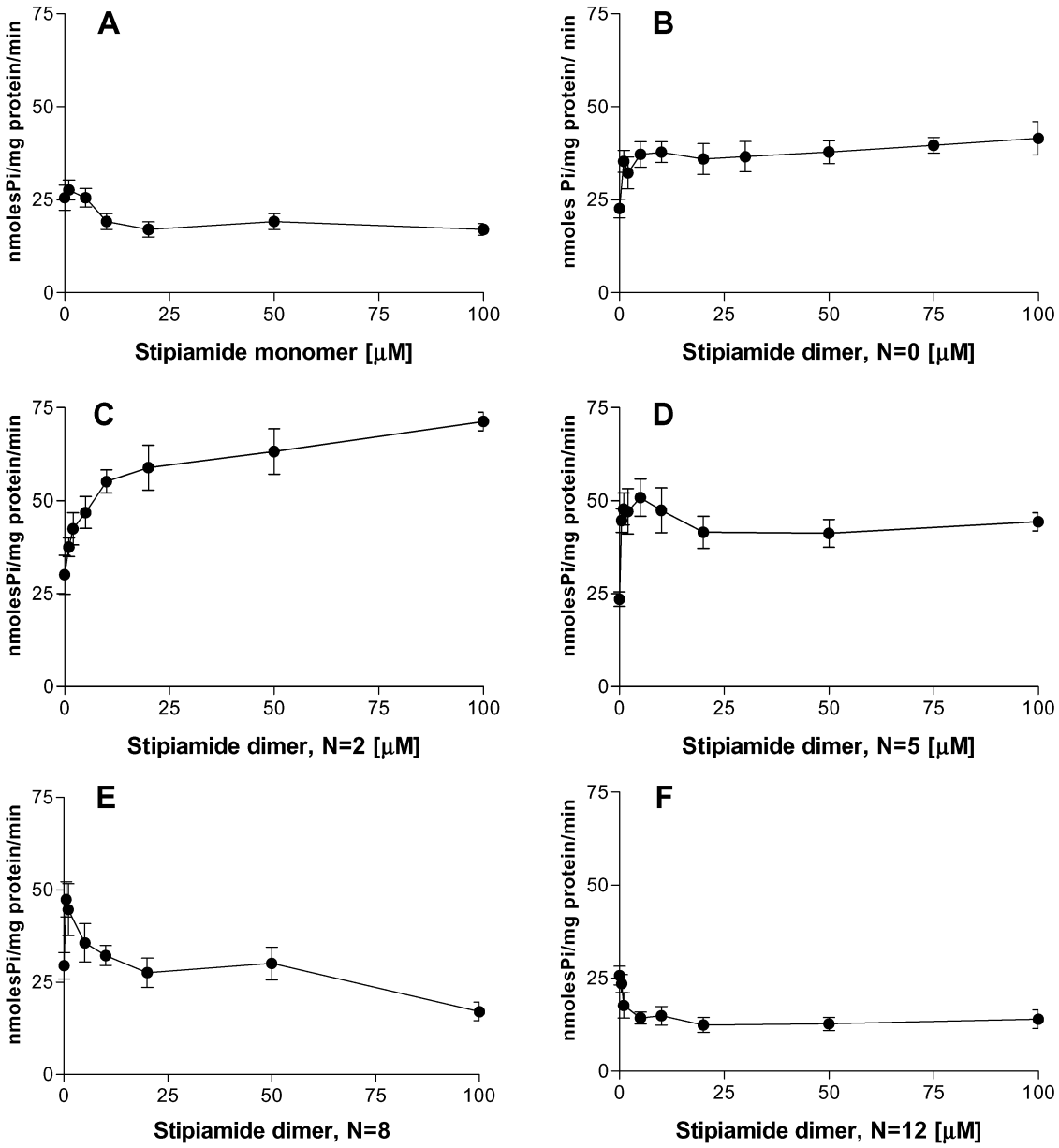


FIGURE 3: Effect of the stipiamide monomer and dimers on the ATP hydrolysis by Pgp. Vi-sensitive ATP hydrolysis was assessed in Pgp-containing crude membranes prepared from High Five insect cells as described in Experimental Procedures. The graphs show ATP hydrolysis [mean ± the standard deviation ($N = 3$)] in the presence of increasing concentrations of the stipiamide monomer (A) and the dimers separated by 3 (B), 11 (C), 22 (D), 35 (E), and 50 Å linkers (F).

We used a stipiamide monomer with the polyethylene tail as the control in these experiments as our previous work has shown that the addition of this group increases the efficacy of stipiamide (*17*). The spacers had 0, 2, 5, 8, and 12 ethylene glycol ether groups which correspond to distances of 3, 11, 22, 35, and 50 Å, respectively, between the two amide nitrogens.

*Effect of Stipiamide Dimers on the Binding of IAAP to Pgp.* IAAP, the $^{125}$I-labeled azido analogue of the Pgp drug substrate prazosin, is an excellent reagent for directly probing interactions at the drug substrate site of Pgp. IAAP can be photo-cross-linked to the drug substrate site of Pgp and can be visualized as a radioactive band on an SDS−PAGE gel. IAAP is a radiolabeled photoaffinity analogue of the Pgp substrate prazosin. The radiolabeled IAAP is transported by Pgp (*45*); we have previously demonstrated that IAAP shows saturation binding to Pgp, and the Henri−Michaelis−Menten single-site model best described the data (*46*). Moreover, it was demonstrated that this rapid equilibrium approach was deemed appropriate for determining the binding constants $K_d$ and $B_{max}$ as the basic assumptions of the approach were satisfied. (a) The protein and ligand were allowed to interact in the dark, whereby equilibrium conditions existed until the photo-cross-linking step (considered analogous to termination of the reaction). (b) Sufficiently low concentrations of Pgp were used to ensure that the ligand, IAAP, was always in an approximately 100-fold excess. (c) It is necessary to show that the binding is specific at all substrate concentrations. We have determined that cyclosporin A at both low and high concentrations of IAAP (600 and 5 nM, respectively) shows equivalent inhibition of IAAP binding. We have also demonstrated that cyclosporin A inhibits IAAP in a concentration-dependent manner which is independent of the time of irradiation (Z. E. Sauna and S. V. Ambudkar, unpublished

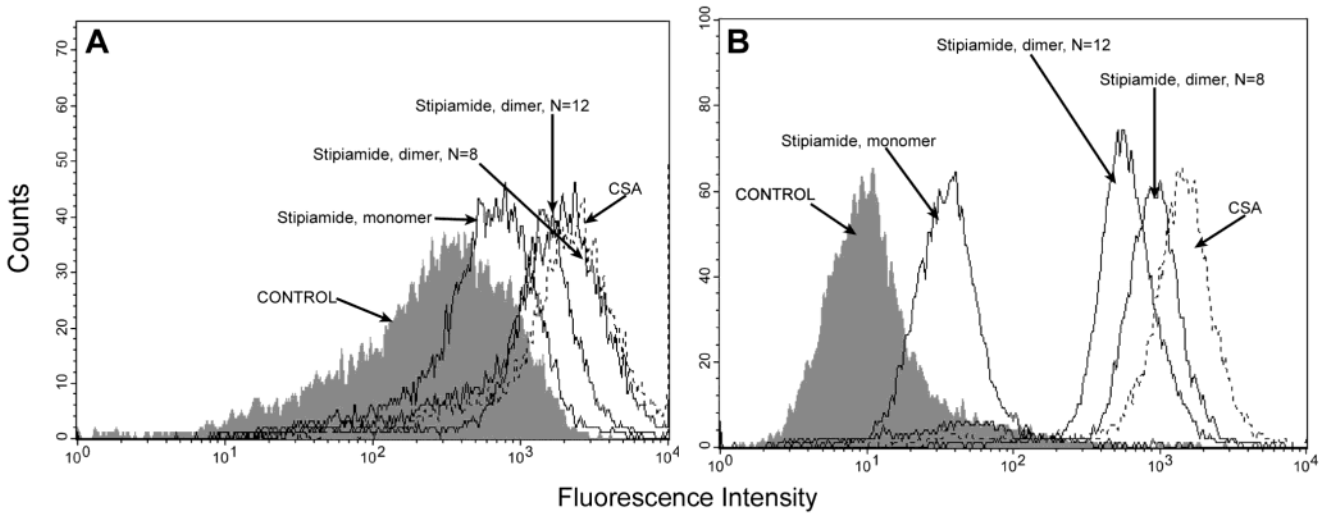


FIGURE 4: Effect of the stipiamide monomer and selected dimers on Pgp-mediated drug efflux. The effect of the stipiamide monomer and selected dimers (with 35 and 50 Å linkers) was monitored in human *MDR*1-expressing NIH-3T3 cells by using Pgp substrates bodipy-FL-prazosin (A) and calcein AM (B) in transport assays. The transport assays were performed using 0.5 $\mu$M bodipy-FL-prazosin or 0.25 $\mu$M calcein AM and analyzed by flow cytometry as described in Experimental Procedures. The histograms show untreated cells (gray, filled histogram) and those treated with 25 $\mu$M stipiamide monomer or dimers. Individual histograms are labeled in the figure. This figure is representative of three independent experiments.

observations). These properties of IAAP can be exploited in computing the relative affinities of compounds for Pgp (*47*). To compare the relative affinities of the stipiamide analogues for Pgp, constant amounts of Pgp and IAAP were allowed to interact in the presence of increasing concentrations of the stipiamide dimers in the dark so that equilibrium conditions exist until the photo-cross-linking step (see above). The samples were then UV irradiated and electrophoresed. Figure 2A shows that when equal amounts of the protein were loaded on the gel, the autoradiogram shows a decreasing radioactive signal associated with the Pgp band. The relative intensities of the radioactive signals were quantified using a phosphorimager, and the percent inhibition was plotted as a function of either the stipiamide monomer or stipiamide dimer concentration (Figure 2B−G). The fact that the data for each stipiamide dimer fit the Henri−Michaelis−Menten equation suggests direct competition for the IAAP binding site at a single site rather than an allosteric interaction. Thus, it appears to be reasonable to conclude that the stipiamide dimers displace IAAP from the drug binding pocket. Though the stipiamide monomer and all five stipiamide dimers inhibit IAAP binding, the $IC_{50}$ values vary considerably (Figure 2B−G). Thus, there is a direct correlation between the relative affinity of the dimer and the length of the PEG ether spacer. The $IC_{50}$ for the monomer was 1.1 $\mu$M, and that for the stipiamide dimer ($N = 12$) was 0.1 $\mu$M, a 11-fold increase in affinity. More importantly, at saturating concentrations, the monomer elicits an approximately 50% inhibition of IAAP binding whereas the dimer inhibits >75% of the IAAP binding.

*Effect of Stipiamide Dimers on the Vi-Sensitive ATP Hydrolysis by Pgp.* As ATP hydrolysis and drug transport by Pgp are obligatorily linked, several laboratories have demonstrated that the interaction of drug substrates with Pgp can be monitored via their effect on the ATP hydrolysis (*36*, *48*, *49*). We therefore assessed the ATP hydrolysis by Pgp in the presence of increasing concentrations of the stipiamide dimers. The stipiamide monomer inhibits ATP hydrolysis (Figure 3A), while the dimers with spacer lengths of 3, 11, and 22 Å all stimulate ATP hydrolysis, with the longer spacers exhibiting increased fold stimulation (Figure 3B−D). Dimers with spacers of 35 and 50 Å, on the other hand, strongly inhibit ATP hydrolysis (Figure 3E,F). The effect of spacer length on Pgp-mediated ATP hydrolysis reflects the changes in affinity (see Figure 2 and Discussion).

*Effect of Stipiamide Dimers on the Efflux of Bodipy-Prazosin and Calcein AM by NIH-3T3 Cells Expressing Pgp.* Pgp-mediated efflux of drugs can be monitored using fluorescent derivatives of drug substrates. Thus, for example, the NIH-MDR-G185 cells show significantly reduced levels of accumulation of fluorescent analogues of Pgp drug substrates compared to the parental untransfected NIH-3T3 drug-sensitive cells (*32*−*34*). To distinguish overexpression of human and mouse Pgps in NIH-MDR-G185 cells, Western blots were probed with the C219 monoclonal antibody that reacts with both mouse and human Pgp and the polyclonal antibody PEPG 13 that recognizes only human Pgp (*50*). The signals with both antibodies were comparable in the NIH-MDR-G185 cells, suggesting that these cells do not overexpress the mouse Pgp. In the presence of agents such as cyclosporin A that inhibit Pgp function, the Pgp-overexpressing cells accumulate fluorescent analogues of Pgp substrates at levels comparable to those in the parental cells. We have investigated the effect of the stipiamide monomer and dimers on the efflux of fluorescent drug substrates from Pgp-overexpressing cells. We demonstrate in Figure 4 that the stipiamide monomer and select dimers increase the level of accumulation of bodipy-prazosin as well as calcein in Pgp-expressing NIH-3T3 cells. It, however, is apparent that while both the monomer and the dimers show reversal of Pgp-mediated drug efflux there are quantitative differences. To systematically study the influence of length of the PEG ether spacers on reversal of drug efflux, we used bodipy-prazosin because the previous experiments that estimated the $IC_{50}$ values for the displacement of drug were performed with IAAP, which is a photoaffinity analogue of prazosin. Some of the stipiamide dimers showed a dose-dependent reversal of bodipy-prazosin, while others had little or no effect. Thus,

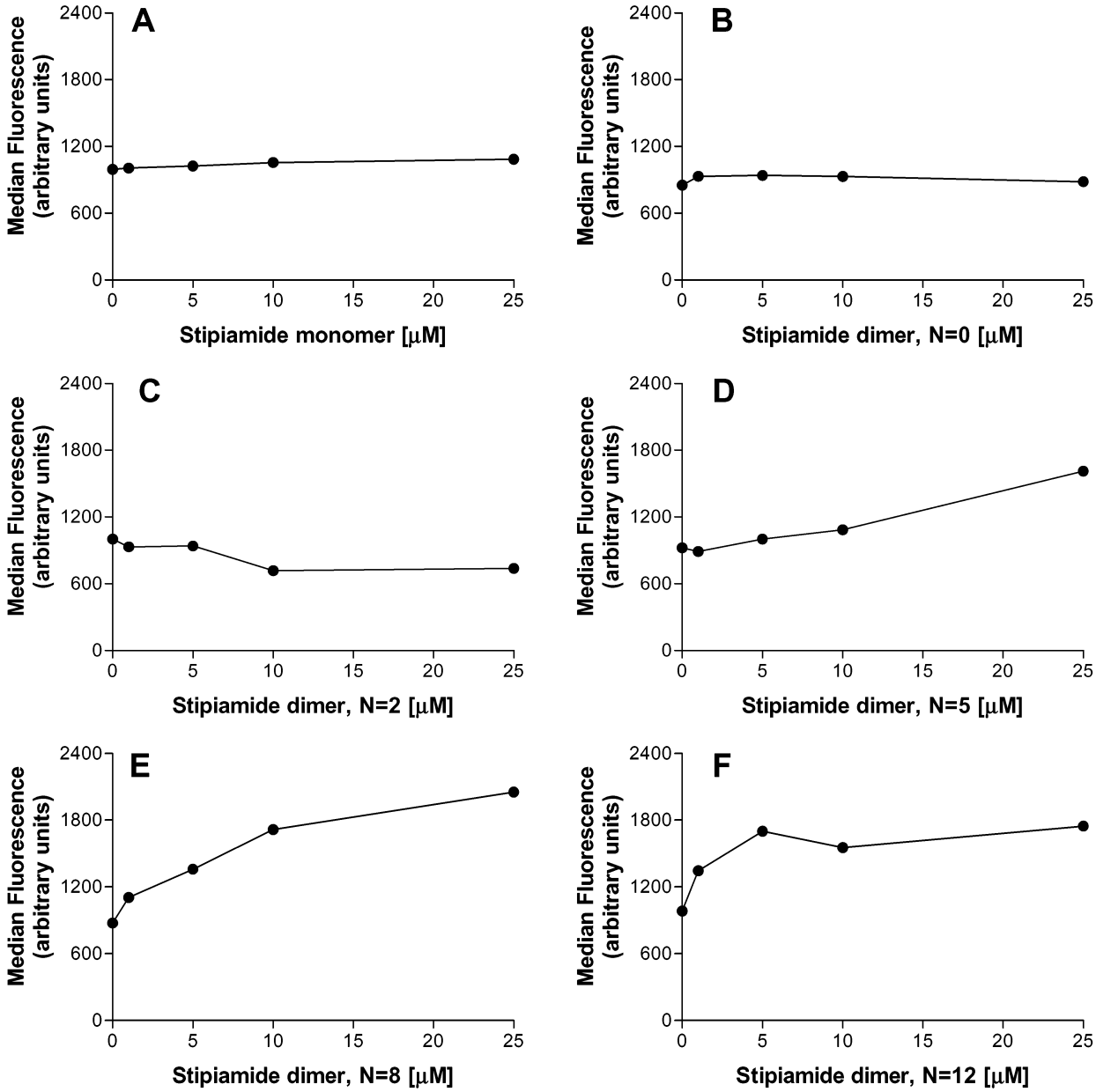


FIGURE 5: Dose-dependent effects of the stipiamide monomer and dimers on the transport of drug substrates by NIH-3T3 cells expressing the *MDR*1 gene. The effect of the stipiamides was monitored in human *MDR*1-expressing NIH-3T3 cells by using Pgp substrate bodipy-FL-prazosin in a transport assay. The transport assay was performed using 0.5 $\mu$M bodipy-FL-prazosin and analyzed by flow cytometry as described in Experimental Procedures. After the flow cytometric assay had been performed, the median fluorescence at each concentration of the modulator was determined from histogram plots similar to the ones depicted in Figure 4 using Cell Quest. The plots depict the median fluorescence as a function of the increasing concentration of the stipiamide monomer (A) and the dimers with 3 (B), 11 (C), 22 (D), 35 (E), and 50 Å linkers (F). One of three independent experiments is depicted.

in Figure 5, we depict the median fluorescence in a population of Pgp-overexpressing cells as a function of increasing concentrations of the stipiamides. We observed that the stipiamide monomer and the dimers with the short spacers [3 and 11 Å ($N = 0$ and 2)] had a negligible effect on the accumulation of bodipy-prazosin in Pgp-overexpressing NIH-MDR-G185 cells (Figure 5A−C). Spacers longer than this threshold appeared to increase the level of accumulation (Figure 5D,E) of bodipy-prazsion. However, this increase in the level of accumulation of the fluorophore appeared to plateau with spacers larger than 35 Å, i.e., $N = 8$ (Figure 5E,F). Control NIH-3T3 cells exhibit accumulation of bodipy-prazosin which is not affected by cyclosporin A or any of the stipiamide derivatives tested in this work (data not given). These results confirm earlier reports that stipiamide analogues interact with Pgp (*14*, *17*, *51*) and suggest that dimerization with a spacer of the optimal length can augment the reversal of Pgp-mediated drug resistance.

*Effect of Stipiamide Dimers on the Binding of [α-$^{32}$P]-8-AzidoATP to Pgp.* The results depicted above indicate that the homodimers of stipiamide interact with the drug binding site and affect drug transport and ATP hydrolysis as a consequence. There, however, does exist the possibility that these dimers interact directly with the ATP site(s) of Pgp. To test this possibility, we monitored the binding of the photoaffinity analogue of ATP, [α-$^{32}$P]-8-azidoATP, in the presence of a saturating concentration (25 $\mu$M) of each of the dimers. Figure 6 shows that while ATP completely

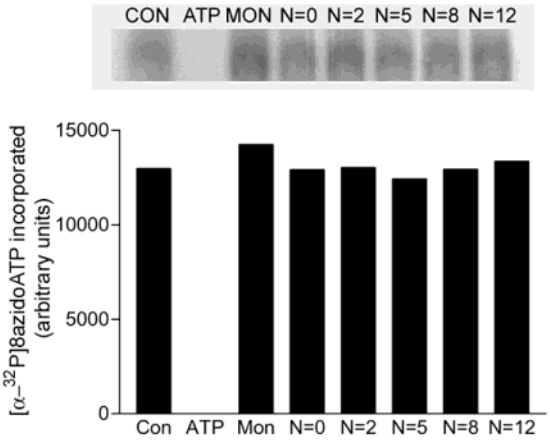


FIGURE 6: Effect of the stipiamide monomer and dimers on the binding of [α-$^{32}$P]-8-azidoATP to Pgp. The binding of [α-$^{32}$P]-8-azidoATP (10 $\mu$M, 10 $\mu$Ci/nmol) was assessed as described in Experimental Procedures at 4 °C (under nonhydrolysis conditions), in the presence of monomer and stipiamide dimers with 3, 11, 22, 35, and 50 Å linkers. All the modulators were used at a concentration of 25 $\mu$M. The experimental conditions are depicted on the autoradiogram. The data from a representative autoradiogram ($N$ = 3) were quantified using a phosphorimager and are plotted in the bottom panel.

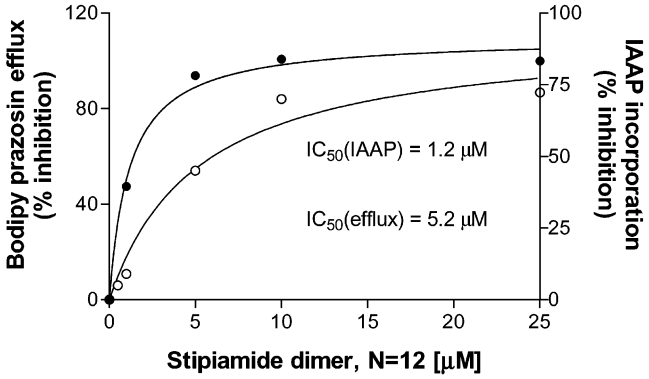


FIGURE 7: Inhibition of IAAP binding and bodipy-prazosin efflux in intact cells. The effect of the stipiamide dimer ($N$ = 12) was monitored in human *MDR*1-expressing NIH-3T3 cells by measuring both the efflux of bodipy-FL-prazosin in a transport assay and the binding of IAAP. The transport assay was performed as described in the legend of Figure 5, and the effect on IAAP binding was assessed as described in Experimental Procedures. The results were quantified and analyzed as described in the legends of Figures 2 and 5 and depict the inhibition of IAAP binding (●) and bodipy-prazosin efflux (○).

abolishes the cross-linking of [α-$^{32}$P]-8-azidoATP to Pgp, none of the stipiamides has a significant effect. It is thus unlikely that either the monomer or the dimeric stipiamides directly bind at the ATP binding sites of Pgp.

*Stipiamide Dimers Inhibit both the Binding of IAAP to Pgp and Fluorescent Drug Efflux in Intact Cells.* The results depicted above indicate that the stipiamide dimers inhibit the binding of IAAP, the photoaffinity analogue of the Pgp drug substrate, prazosin in crude membrane preparations (Figure 2) and also reverse Pgp-mediated drug efflux in intact cells (Figure 5). However, the $IC_{50}$ for the reversal of drug efflux is considerably higher than that for the inhibition of IAAP binding. We therefore assessed both these phenomena in intact cells under identical conditions for a more accurate comparison. The results depicted in Figure 7 show that the stipiamide dimer ($N$ = 12) inhibits the binding of IAAP to Pgp in intact cells with an $IC_{50}$ of 1.2 $\mu$M and inhibits reversal of bodipy-prazosin efflux with an $IC_{50}$ of 5.2 $\mu$M (which are comparable). The increased $IC_{50}$ for the inhibition of IAAP binding in intact cells (0.1 $\mu$M vs 1.2 $\mu$M) probably is related to the delivery of the stipiamides and/or hydrophobic proteins and organelles in intact cells providing a sink for these compounds.

## DISCUSSION

The decreased influx and or increased efflux of chemotherapeutic agents from cancer cells, mediated by molecular pumps powered by ATP hydrolysis, is responsible for MDR (*52*). Overexpression of Pgp is a negative prognostic marker during cancer chemotherapy, and the pharmacological reversal of Pgp function has been a major focus of research for more than 15 years (*53*, *54*). However, success in overcoming MDR has been limited (for a review, see ref *9*). Many of the problems associated with the development of effective agents for combating Pgp-mediated MDR may be traced to a lack of specificity and a low affinity for the drug binding site(s) of Pgp, and several new drugs in clinical trials address some of these problems (*9*, *53*). In this study, we have used dimers of stipiamide that differ in the length of a PEG ether to investigate whether polyvalency is a viable strategy for enhancing the biological activity of Pgp modulators. We have characterized these dimers vis-à-vis Pgp-mediated transport, ATP hydrolysis, and their ability to displace the photoaffinity analogue of the Pgp drug substrate IAAP.

Flow cytometry using fluorescent analogues of Pgp drug substrates offers a rapid means of monitoring the effect of modulators on Pgp-mediated transport (*32*−*34*). The NIH-MDR-G185 cells expressing the *MDR*1 gene show a significantly reduced level of accumulation of bodipy-prazosin due to efflux of the drug by Pgp. This can be reversed by the addition of cyclosporin A (a reversal agent) to obtain a maximal level of bodipy-prazosin accumulation (data not given). The stipiamide monomer alone shows a modest increase in the level of accumulation of calcein or bodipy-prazosin (Figures 4 and 5A). Similarly, dimerization *per se* does not reverse the drug efflux (Figure 5B). This observation also argues against the idea that the increased hydrophobicity of the compounds as a result of adding the PEG ethers could explain the increased activity of the dimers. As depicted in Table 1, there is a sharp increase in the calculated LogP value on dimerization. The homodimers, however, all have comparable LogP values in the range of 10−12. Increasing the length of the spacer between the two monomers on the other hand significantly enhances the accumulation of bodipy-prazosin in the MDR resistant cells by inhibiting the efflux (Figure 5). There is also a decrease in the $K_m$ for the reversal of drug efflux with an increase in spacer length. To quantify these effects, we plotted the extent of reversal as a function of spacer length (Figure 8). Such a plot shows that a spacer of up to 11 Å ($N$ = 2) has no effect on reversal of bodipy-prazosin efflux by *MDR*1-expressing cells. Increasing the spacer length beyond 11 Å increases the capacity of the dimer to inhibit drug efflux in a concentration-dependent manner. Longer spacers in excess of 35 Å ($N$ = 8) do not increase the effectiveness of the dimer. We obtained similar results when we used the calcein AM instead of bodipy-prazosin (Figure 4B), suggesting that

Table 1: Effect of Spacer Length in the Stipiamide Dimers on Pgp-Mediated ATP Hydrolysis, Inhibition of IAAP Binding, and Bodipy-Prazosin Efflux

| | molecular weight | calculated LogP | spacer length (Å)[a] | ATP hydrolysis[b] fold stimulation | ATP hydrolysis[b] fold inhibition | IAAP binding, $IC_{50}$ ($\mu$M)[c] | drug efflux[d] ($\Delta$) |
|---|---|---|---|---|---|---|---|
| monomer control | 679 | 4.7 | – | 1.08 | – | 1.1 | 103 |
| stipiamide dimer ($N = 0$) | 857 | 11.7 | 3 | 1.84 | – | >100 | 88 |
| stipiamide dimer ($N = 2$) | 944 | 11.3 | 11 | 2.37 | – | >100 | 0 |
| stipiamide dimer ($N = 5$) | 1076 | 11.2 | 22 | 1.88 | – | 12.3 | 689 |
| stipiamide dimer ($N = 8$) | 1208 | 10.5 | 35 | – | 0.58 | 0.9 | 1179 |
| stipiamide dimer ($N = 12$) | 1384 | 10.2 | 50 | – | 0.54 | 0.1 | 765 |

[a] Distance between the amide nitrogens of the stipiamide monomers. [b] The Vi-sensitive ATPase activity was determined as described in Experimental Procedures. The fold stimulation or inhibition over basal activity was determined at the steady state. The maximal fold stimulation or inhibition by the stipiamide dimer is given. [c] The $IC_{50}$ values for the inhibition of IAAP binding by the stipiamide dimers were determined as described in the legend of Figure 2. [d] Bodipy-Prazosin efflux was determined in NIH-3T3 cells as described in the legend of Figure 4. The $\Delta$ value refers to the increase in the median fluorescence as a result of the addition of the stipiamide analogue at a saturating concentration.

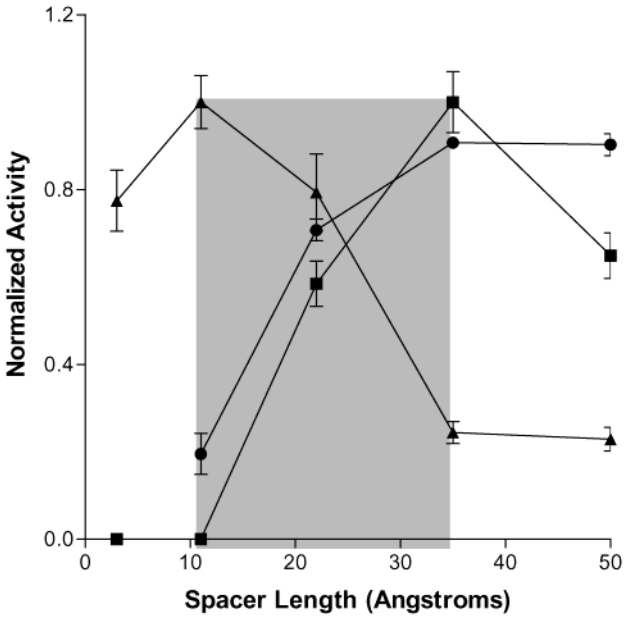


FIGURE 8: Influence of the spacer length in the stipiamide homodimers on IAAP binding, ATP hydrolysis, and drug efflux by Pgp. The following parameters were plotted as a function of the length of the spacer (in angstroms). (i) For IAAP binding, the maximal inhibition of binding of IAAP to Pgp (●). (ii) For ATP hydrolysis, the fold change (stimulation or inhibition) over basal ATPase activity of Pgp at saturating concentrations of the stipiamide (▲). (iii) For efflux of bodipy-prazosin, the increase in the median fluorescence of bodipy-prazosin in Pgp-expressing NIH-3T3 cells expressing the *MDR*1 gene in the presence of the indicated stipiamide dimers (■). Each of the three sets was normalized to facilitate comparison on a common scale. The means ± the standard deviation ($N = 3$) were determined after normalizing the data. All three parameters exhibit a linear relationship for spacers between 11 and 35 Å (shaded area). See the text for an interpretation.

the stipiamide analogues have equivalent effects regardless of the nature of the fluorescent substrate used to track Pgp-mediated efflux.

To obtain a comprehensive understanding of the effect of spacer length in stipamide dimers at the biochemical level, we studied ATP hydrolysis and drug substrate binding. The effects of the stipiamide monomer and dimers on Pgp function are summarized in Table 1. IAAP, a radiolabeled photoaffinity analogue of the Pgp substrate prazosin, has been extensively used to study the drug binding sites of Pgp (*18*, *46*, *55*, *56*). Modulators that compete for the drug binding site of Pgp inhibit the photoaffinity labeling of IAAP by Pgp. Figure 2 and Table 1 show that the stipiamide monomer and all the stipiamide dimers inhibit the binding of IAAP to Pgp in a concentration-dependent manner. However, the $IC_{50}$ values vary from >100 to 0.1 $\mu$M. Consistent with the results depicted above, there is a linear decrease in $IC_{50}$ values as the spacer length increases from 11 to 35 Å (from $N = 2$ to $N = 12$, respectively), after which the decrease levels off. Finally, the effect of spacer length on Pgp-mediated ATP hydrolysis can be explained on the basis of the relative affinities of the dimers.

As one increases the length of the spacer from 11 to 35 Å (from $N = 2$ to $N = 8$, respectively), there is an exponential increase in the affinity of the stipiamide dimers for Pgp. The effect of these dimers on ATP hydrolysis is a little more complex; one initially observes an increase in the fold stimulation over basal activity followed by a decrease in the extent of stimulation. This is consistent with the notion that modulators that are bulky or bind too tightly to Pgp are not easily transported from the "on" to the "off" site and thus inhibit ATP hydrolysis. These observations are for example comparable with what has been reported vis-à-vis cyclosporin A (*57*). Finally, we see that increased affinity of the dimers is qualitatively reflected in the reversal of Pgp-mediated drug efflux. Moreover, when we compare both inhibition of IAAP binding and drug efflux in intact cells, the $IC_{50}$ values are in the same range (Figure 7). Thus, when we plot reversal of drug efflux, ATP hydrolysis, and inhibition of IAAP binding as a function of the length of the PEG ether spacer (Figure 8), we observe a consistent pattern. The largest changes in diverse biochemical parameters that define Pgp function occur when the spacer length is increased from 11 to 35 Å (from $N = 2$ to $N = 8$, respectively), the area that has been shaded in Figure 8. How do these findings relate to our current understanding of the drug binding site(s) of Pgp?

Several authors have proposed that there are at least two and possibly several overlapping drug binding sites in Pgp (*18*, *19*, *21*, *58*) and that some modulators may operate more efficiently as pairs (*22*, *23*). What is not clear is whether these are distinct sites or part of a single drug binding pocket. X-ray crystallographic studies with bacterial multidrug binding proteins favor the latter scenario. Thus, the structure of QacR, a soluble regulatory protein from *Staphylococcus aureus*, indicates the presence of two separate potentially overlapping binding sites within a single pocket (*59*). More recently, the X-ray crystallographic structures of the trimeric

AcrB transporter from *Escherichia coli* have been obtained with four structurally diverse ligands (*60*). The structures show that three molecules of ligands bind simultaneously to the extremely large central cavity and each ligand uses a slightly different subset of AcrB residues. Our finding that dimerization of stipiamide using spacers of a defined spacer length increases the affinity more than 25-fold would support such a drug binding site for Pgp. Multiple binding sites are necessary for polyvalency to succeed. However, that dimerization *per se* does not increase the affinity of stipiamide suggests that the dimer requires structural flexibility to associate with the multiple binding sites within the drug binding site of Pgp. Such a view is supported by a recent report that demonstrates the simultaneous binding of two different drugs in the binding pocket of the human Pgp (*38*). Moreover, the critical spacer length of 11−35 Å (see Figure 8 for a comparison of the effect of spacer length on different biochemical parameters) is also consistent with the emerging insights into the Pgp drug binding site. Using a series of methanethiosulfonate cross-linkers with spacer arms of 2−17 atoms in conjugation with cysteine mutagenesis, Loo and Clarke have estimated the drug binding site of Pgp is funnel-shaped, and is 9−25 Å in length (*39*). This is consistent with our results where we observe improved binding, with spacers of 11−35 Å. Shorter spacers either do not allow the stipiamide dimer sufficient flexibility or do not permit the interactions between both the stipiamides and the requisite amino acid residues in the drug binding site. Very large spacers (>35 Å), on the other hand, increase the bulk of the molecule to the extent that it no longer fits in the drug binding site.

Our results thus support the emerging postulate that Pgp, akin to multidrug transport proteins from bacteria, may possess multiple drug binding sites within a common pocket (*59*, *60*). Where such proteins are the targets of clinical intervention, polyvalency would offer a powerful means of designing more efficient drugs. We provide a proof of principle for this approach by demonstrating a >10-fold increase in the affinity of stipiamide for Pgp achieved by generating dimers separated by an optimal spacer length. Increasing the potency of MDR modulators is fundamental to generating effective modulators while keeping side effects manageable (*9*). Though significant strides in achieving this objective have been made in recent years, there are no modulators of MDR available for clinical use. This work characterizes polyvalency as a general strategy for increasing the potency of MDR modulators and provides an important new tool for addressing this significant clinical problem.

## ACKNOWLEDGMENT

We thank Dr. Michael M. Gottesman for encouragement and for comments on the manuscript and Dr. Wilfred D. Stein for help with data analysis and discussions. We are grateful to Carol Cardarelli for providing us with cells, In Wha Kim for help with flow cytometry, and Jen McCulley for technical help.

## REFERENCES

1. Gottesman, M. M., Pastan, I., and Ambudkar, S. V. (1996) P-glycoprotein and multidrug resistance, *Curr. Opin. Genet. Dev. 6*, 610−617.
2. Sauna, Z. E., Smith, M. M., Muller, M., Kerr, K. M., and Ambudkar, S. V. (2001) The mechanism of action of multidrug-resistance-linked P-glycoprotein, *J. Bioenerg. Biomembr. 33*, 481−491.
3. Gottesman, M. M., and Pastan, I. (1993) Biochemistry of multidrug resistance mediated by the multidrug transporter, *Annu. Rev. Biochem. 62*, 385−427.
4. Ambudkar, S. V., Dey, S., Hrycyna, C. A., Ramachandra, M., Pastan, I., and Gottesman, M. M. (1999) Biochemical, cellular, and pharmacological aspects of the multidrug transporter, *Annu. Rev. Pharmacol. Toxicol. 39*, 361−398.
5. Ford, J. M., and Hait, W. N. (1990) Pharmacology of drugs that alter multidrug resistance in cancer, *Pharmacol. Rev. 42*, 155−199.
6. Seelig, A. (1998) How does P-glycoprotein recognize its substrates? *Int. J. Clin. Pharmacol. Ther. 36*, 50−54.
7. Seelig, A. (1998) A general pattern for substrate recognition by P-glycoprotein, *Eur. J. Biochem. 251*, 252−261.
8. Ecker, G., Huber, M., Schmid, D., and Chiba, P. (1999) The importance of a nitrogen atom in modulators of multidrug resistance, *Mol. Pharmacol. 56*, 791−796.
9. Gottesman, M. M., Fojo, T., and Bates, S. E. (2002) Multidrug resistance in cancer: Role of ATP-dependent transporters, *Nat. Rev. Cancer 2*, 48−58.
10. Gottesman, M. M. (2002) Mechanisms of drug resistance, *Annu. Rev. Med. 53*, 615−627.
11. Persidis, A. (1999) Cancer multidrug resistance, *Nat. Biotechnol. 17*, 94−95.
12. Andrus, M. B., Lepore, S. D., and Turner, T. M. (1997) Total synthesis of stipiamide and designed polyenes as new agents for the reversal of multidrug resistance, *J. Am. Chem. Soc. 119*, 12159−12169.
13. Andrus, M. B., Turner, T. M., Asgari, D., and Li, W. K. (1999) The synthesis and evaluation of a solution-phase indexed combinatorial library of non-natural polyenes for multidrug resistance reversal, *J. Org. Chem. 64*, 2978−2979.
14. Andrus, M. B., Turner, T. M., Sauna, Z. E., and Ambudkar, S. V. (2000) The synthesis and evaluation of a solution phase indexed combinatorial library of non-natural polyenes for reversal of P-glycoprotein mediated multidrug resistance, *J. Org. Chem. 65*, 4973−4983.
15. Kim, Y. J., Furihata, K., Yamanaka, S., Fudo, R., and Seto, H. (1991) Isolation and structural elucidation of stipiamide, a new antibiotic effective to multidrug-resistant cancer cells, *J. Antibiot. 44*, 553−555.
16. Andrus, M. B., and Lepore, S. D. (1997) Synthesis of stipiamide and a new multidrug resistance reversal agent, 6,7-dehydrostipiamide, *J. Am. Chem. Soc. 119*, 2327−2328.
17. Andrus, M. B., Turner, T. M., Updegraff, E. P., Sauna, Z. E., and Ambudkar, S. V. (2001) Synthesis and analysis of polyethylene glycol linked P-glycoprotein-specific homodimers based on (−)-stipiamide, *Tetrahedron Lett. 42*, 3819−3822.
18. Dey, S., Ramachandra, M., Pastan, I., Gottesman, M. M., and Ambudkar, S. V. (1997) Evidence for two nonidentical drug-interaction sites in the human P-glycoprotein, *Proc. Natl. Acad. Sci. U.S.A. 94*, 10594−10599.
19. Shapiro, A. B., and Ling, V. (1997) Positively cooperative sites for drug transport by P-glycoprotein with distinct drug specificities, *Eur. J. Biochem. 250*, 130−137.
20. Shapiro, A. B., and Ling, V. (1997) Extraction of hoechst 33342 from the cytoplasmic leaflet of the plasma membrane by P-glycoprotein, *Eur. J. Biochem. 250*, 122−129.
21. Shapiro, A. B., and Ling, V. (1998) Transport of LDS-751 from the cytoplasmic leaflet of the plasma membrane by the rhodamine-123-selective site of P-glycoprotein, *Eur. J. Biochem. 254*, 181−188.
22. Ayesh, S., Shao, Y. M., and Stein, W. D. (1996) Co-operative, competitive and non-competitive interactions between modulators of P-glycoprotein, *Biochim. Biophys. Acta 1316*, 8−18.
23. Litman, T., Zeuthen, T., Skovsgaard, T., and Stein, W. D. (1997) Competitive, non-competitive and cooperative interactions between substrates of P-glycoprotein as measured by its ATPase activity, *Biochim. Biophys. Acta 1361*, 169−176.
24. Matrosovich, M. N. (1989) Towards the development of antimicrobial drugs acting by inhibition of pathogen attachment to host cells: a need for polyvalency, *FEBS Lett. 252*, 1−4.
25. Crabtree, G. R., and Schreiber, S. L. (1996) Three-part inventions: Intracellular signaling and induced proximity, *Trends Biochem. Sci. 21*, 418−422.

26. Rao, J. H., Lahiri, J., Isaacs, L., Weis, R. M., and Whitesides, G. M. (1998) A trivalent system from vancomycin·D-Ala-D-Ala with higher affinity than avidin·biotin, *Science 280*, 708−711.
27. Williams, D. H., Maguire, A. J., Tsuzuki, W., and Westwell, M. S. (1998) An analysis of the origins of a cooperative binding energy of dimerization, *Science 280*, 711−714.
28. Sundram, U. N., Griffin, J. H., and Nicas, T. I. (1996) Novel vancomycin dimers with activity against vancomycin-resistant enterococci, *J. Am. Chem. Soc. 118*, 13107−13108.
29. Schafer, M., Schneider, T. R., and Sheldrick, G. M. (1996) Crystal structure of vancomycin, *Structure 4*, 1509−1515.
30. Cooper, A., and McAuleyhecht, K. E. (1993) Microcalorimetry and the molecular recognition of peptides and proteins, *Philos. Trans. R. Soc. London, Ser. A 345*, 23−35.
31. Cardarelli, C. O., Aksentijevich, I., Pastan, I., and Gottesman, M. M. (1995) Differential effects of P-glycoprotein inhibitors on NIH3T3 cells transfected with wild-type (G185) or mutant (V185) multidrug transporters, *Cancer Res. 55*, 1086−1091.
32. Hrycyna, C. A., Ramachandra, M., Pastan, I., and Gottesman, M. M. (1998) Functional expression of human P-glycoprotein from plasmids using vaccinia virus-bacteriophage T7 RNA polymerase system, *Methods Enzymol. 292*, 456−473.
33. Ramachandra, M., Ambudkar, S. V., Gottesman, M. M., Pastan, I., and Hrycyna, C. A. (1996) Functional characterization of a glycine 185-to-valine substitution in human P-glycoprotein by using a vaccinia-based transient expression system, *Mol. Biol. Cell 7*, 1485−1498.
34. Gribar, J. J., Ramachandra, M., Hrycyna, C. A., Dey, S., and Ambudkar, S. V. (2000) Functional characterization of glycosylation-deficient human P-glycoprotein using a vaccinia virus expression system, *J. Membr. Biol. 173*, 203−214.
35. Ramachandra, M., Ambudkar, S. V., Chen, D., Hrycyna, C. A., Dey, S., Gottesman, M. M., and Pastan, I. (1998) Human P-glycoprotein exhibits reduced affinity for substrates during a catalytic transition state, *Biochemistry 37*, 5010−5019.
36. Sarkadi, B., Price, E. M., Boucher, R. C., Germann, U. A., and Scarborough, G. A. (1992) Expression of the human multidrug resistance cDNA in insect cells generates a high activity drug-stimulated membrane ATPase, *J. Biol. Chem. 267*, 4854−4858.
37. Sauna, Z. E., and Ambudkar, S. V. (2001) Characterization of the catalytic cycle of ATP hydrolysis by human P-glycoprotein: The two ATP hydrolysis events in a single catalytic cycle are kinetically similar but affect different functional outcomes, *J. Biol. Chem. 276*, 11653−11661.
38. Loo, T. W., Bartlett, M. C., and Clarke, D. M. (2003) Simultaneous binding of two different drugs in the binding pocket of the human multidrug resistance P-glycoprotein, *J. Biol. Chem. 278*, 39706−39710.
39. Loo, T. W., and Clarke, D. M. (2001) Defining the drug-binding site in the human multidrug resistance P-glycoprotein using a methanethiosulfonate analog of verapamil, MTS-verapamil, *J. Biol. Chem. 276*, 14972−14979.
40. Rao, J. H., Yan, L., Lahiri, J., Whitesides, G. M., Weis, R. M., and Warren, H. S. (1999) Binding of a dimeric derivative of vancomycin to L-Lys-D-Ala-D-lactate in solution and at a surface, *Chem. Biol. 6*, 353−359.
41. Kanai, M., Mortell, K. H., and Kiessling, L. L. (1997) Varying the size of multivalent ligands: The dependence of concanavalin a binding on neoglycopolymer length, *J. Am. Chem. Soc. 119*, 9931−9932.
42. Mistry, P., Stewart, A. J., Dangerfield, W., Okiji, S., Liddle, C., Bootle, D., Plumb, J. A., Templeton, D., and Charlton, P. (2001) In vitro and in vivo reversal of P-glycoprotein-mediated multidrug resistance by a novel potent modulator, XR9576, *Cancer Res. 61*, 749−758.
43. Dantzig, A. H., Law, K. L., Cao, J., and Starling, J. J. (2001) Reversal of multidrug resistance by the P-glycoprotein modulator, LY335979, from the bench to the clinic, *Curr. Med. Chem. 8*, 39−50.
44. Polli, J. W., Baughman, T. M., Humphreys, J. E., Jordan, K. H., Mote, A. L., Salisbury, J. A., Tippin, T. K., and Serabjit-Singh, C. J. (2003) P-Glycoprotein influences the brain concentrations of cetirizine (Zyrtec (R)), a second-generation non-sedating antihistamine, *J. Pharm. Sci. 92*, 2082−2089.
45. Maki, N., Hafkemeyer, P., and Dey, S. (2003) Allosteric modulation of human P-glycoprotein: Inhibition of transport by preventing substrate translocation and dissociation, *J. Biol. Chem. 278*, 18132−18139.
46. Sauna, Z. E., and Ambudkar, S. V. (2000) Evidence for a requirement for ATP hydrolysis at two distinct steps during a single turnover of the catalytic cycle of human P-glycoprotein, *Proc. Natl. Acad. Sci. U.S.A. 97*, 2515−2520.
47. Sauna, Z. E., Peng, X. H., Nandigama, K., Tekle, S., and Ambudkar, S. V. (2003) The molecular basis of the action of disulfiram as a modulator of the multidrug resistance linked ABC transporters MDR1 (ABCB1) and MRP1 (ABCC1), *Mol. Pharmacol.* (in press).
48. Ambudkar, S. V., Lelong, I. H., Zhang, J., Cardarelli, C. O., Gottesman, M. M., and Pastan, I. (1992) Partial purification and reconstitution of the human multidrug-resistance pump: Characterization of the drug-stimulatable ATP hydrolysis, *Proc. Natl. Acad. Sci. U.S.A. 89*, 8472−8476.
49. Scarborough, G. A. (1995) Drug-stimulated ATPase activity of the human P-glycoprotein, *J. Bioenerg. Biomembr. 27*, 37−41.
50. Ambudkar, S. V. (1998) Drug-stimulatable ATPase activity in crude membranes of human MDR1-transfected mammalian cells, *Methods Enzymol. 292*, 504−514.
51. Andrus, M. B., Turner, T. M., Sauna, Z. E., and Ambudkar, S. V. (2000) Synthesis and preliminary analysis of a P-glycoprotein-specific H-3-benzophenone photoaffinity label based on (−)-stipiamide, *Bioorg. Med. Chem. Lett. 10*, 2275−2278.
52. Gottesman, M. M. (2002) Mechanisms of cancer drug resistance, *Annu. Rev. Med. 53*, 615−627.
53. Tan, B., Piwnica-Worms, D., and Ratner, L. (2000) Multidrug resistance transporters and modulation, *Curr. Opin. Oncol. 12*, 450−458.
54. Stein, W. D. (2002) Reversers of the multidrug resistance transporter P-glycoprotein, *Curr. Opin. Invest. Drugs 3*, 812−817.
55. Greenberger, L. M. (1993) Major photoaffinity drug labeling sites for iodoaryl azidoprazosin in P-glycoprotein are within, or immediately C-terminal to, transmembrane domains 6 and 12, *J. Biol. Chem. 268*, 11417−11425.
56. Sauna, Z. E., Smith, M. M., Muller, M., and Ambudkar, S. V. (2001) Evidence for the vectorial nature of drug (substrate)-stimulated ATP hydrolysis by human P-glycoprotein, *J. Biol. Chem. 276*, 33301−33304.
57. Kerr, K. M., Sauna, Z. E., and Ambudkar, S. V. (2001) Correlation between steady-state ATP hydrolysis and vanadate-induced ADP trapping in human P-glycoprotein. Evidence for ADP release as the rate-limiting step in the catalytic cycle and its modulation by substrates, *J. Biol. Chem. 276*, 8657−8664.
58. Shapiro, A. B., Fox, K., Lam, P., and Ling, V. (1999) Stimulation of P-glycoprotein-mediated drug transport by prazosin and progesterone. Evidence for a third drug-binding site, *Eur. J. Biochem. 259*, 841−850.
59. Schumacher, M. A., Miller, M. C., Grkovic, S., Brown, M. H., Skurray, R. A., and Brennan, R. G. (2001) Structural mechanisms of QacR induction and multidrug recognition, *Science 294*, 2158−2163.
60. Yu, E. W., McDermott, G., Zgurskaya, H. I., Nikaido, H., and Koshland, D. E. (2003) Structural basis of multiple drug-binding capacity of the AcrB multidrug efflux pump, *Science 300*, 976−980.


BI035965K